

VIP Very Important Paper

CHEM  
TALENTS  
BIO

# Orthogonally Stimulated Assembly/Disassembly of Depsipeptides by Rational Chemical Design

Michaela Pieszka,<sup>[a, b]</sup> Adriana Maria Sobota,<sup>[a]</sup> Jasmina Gačanin,<sup>[a, b]</sup> Tanja Weil,<sup>\*[a, b]</sup> and David Y. W. Ng<sup>\*[a]</sup>

Controlling the assembly and disassembly of cross- $\beta$ -sheet-forming peptides is one of the predominant challenges for this class of supramolecular material. As they constitute a continuously propagating material, every atomic change can be exploited to bring about distinct responses at the architectural level. We report herein that, by using rational chemical design, serine and methionine can both be used as orthogonal chemical triggers to signal assembly/disassembly through their corresponding stimuli. Serine is used to construct an ester-bond oligopeptide that can undergo O,N-acyl rearrangement, whereas methionine is sensitive to oxidation by H<sub>2</sub>O<sub>2</sub>. Using the example peptide sequence, KIKISQINM, we demonstrate that assembly and disassembly can be independently controlled on demand.

The molecular ordering of small molecules formed by regular and precise intermolecular forces represents one of the leading principles of supramolecular material synthesis.<sup>[1]</sup> Programmed through molecular design, these interactions involve a selection of hydrogen bonds,  $\pi$ -stacks, and van der Waals as well as electrostatic forces in which self-association of the molecules is often a thermodynamic minimum.<sup>[1]</sup> As it is coupled with the release of solvent molecules, the assembly is also driven entropically and, thus, derives its innate sensitivity towards both temperature and the concentration of the monomers.<sup>[2]</sup> As these various parameters can all affect self-assembly, it can often be a challenge to exert direct control over the kinetics and responsiveness of superstructure formation.

Among different self-assembling systems, the cross- $\beta$ -sheet arrangement of many peptides, which forms so-called amyloid

structures, has emerged a major class of nanomaterials with several unique features. Amyloid structures are often associated with severe neurodegenerative disorders such as Alzheimer's disease.<sup>[3]</sup> The propagation of the disease stems from several known oligopeptide sequences that exhibit a very strong tendency to form cross- $\beta$ -sheets that subsequently assemble into hierarchical fibrillary networks.<sup>[4]</sup> Although the accumulation of these fibrils into larger aggregates can be detrimental to neurons, they have been exploited as excellent molecular support in both nano- and bulk materials, especially when targeted to biomedical applications.<sup>[3,5]</sup>

Nonetheless, the processability as well as temporal control over the self-assembly and disassembly of amyloid-like peptides are prominent limitations to their use in vivo. Hence, significant efforts have been directed towards the design of oligopeptides to allow a higher level of control of  $\beta$ -sheet formation.<sup>[6]</sup> Hydrophilic amino acids within the sequence, such as lysine or glutamic acid, can be leveraged to promote or inhibit intermolecular interactions depending on their protonation state.<sup>[7]</sup> On the other hand, depsipeptides, in which a serine residue within the peptide sequence is connected through an ester bond instead, have shown exceptional promise for amyloid fibril formation by an external pH stimulus.<sup>[8]</sup>

Depsipeptides were originally developed to alleviate solubility issues with ultra-long peptides by providing a kink in the otherwise linear structure.<sup>[9]</sup> This kink, caused by the ester-linked serine residue, would undergo an five-membered O,N-acyl shift due to the higher nucleophilicity of the free amine upon deprotection to furnish the designated peptide. Hence, we envisioned that, depending on the mechanism to release the free amine, the O,N-acyl shift could be controlled covalently on demand.

Likewise, the disassembly of amyloids is a concern for the development of biomaterials, especially for use in vivo.<sup>[10]</sup> The degradation of these systems is essential for their extrusion once their designated purpose has been achieved. However, the disassembly of typical amyloids under physiological conditions is highly unfavourable due to their thermodynamic stability; they are widely known to be heat and proteolytically resistant.<sup>[11]</sup>

To overcome this, we demonstrate that orthogonal chemical triggers can be rationally designed and incorporated within an oligopeptide such that the assembly/disassembly can be controlled independently by external stimuli (Figure 1). We introduced a depsipeptide sequence containing a boronic acid-carbamate bond to cage the amine of the serine. The self-assembling sequence of the oligopeptide contains a methionine resi-

[a] M. Pieszka, A. M. Sobota, J. Gačanin, Prof. Dr. T. Weil, Dr. D. Y. W. Ng  
Synthesis of Macromolecules  
Max Planck Institute for Polymer Research  
Ackermannweg 10, 55128 Mainz (Germany)  
E-mail: weil@mpip-mainz.mpg.de  
david.ng@mpip-mainz.mpg.de

[b] M. Pieszka, J. Gačanin, Prof. Dr. T. Weil  
Institute of Inorganic Chemistry I, Ulm University  
Albert-Einstein-Allee-11, 89081 Ulm (Germany)

Supporting information and the ORCID identification numbers for the authors of this article can be found under <https://doi.org/10.1002/cbic.201800781>.

© 2019 The Authors. Published by Wiley-VCH Verlag GmbH & Co. KGaA. This is an open access article under the terms of the Creative Commons Attribution Non-Commercial License, which permits use, distribution and reproduction in any medium, provided the original work is properly cited and is not used for commercial purposes.

This article is part of the young researchers' issue ChemBioTalents. To view the complete issue, visit <http://chembiochem.org/chembiotalents>

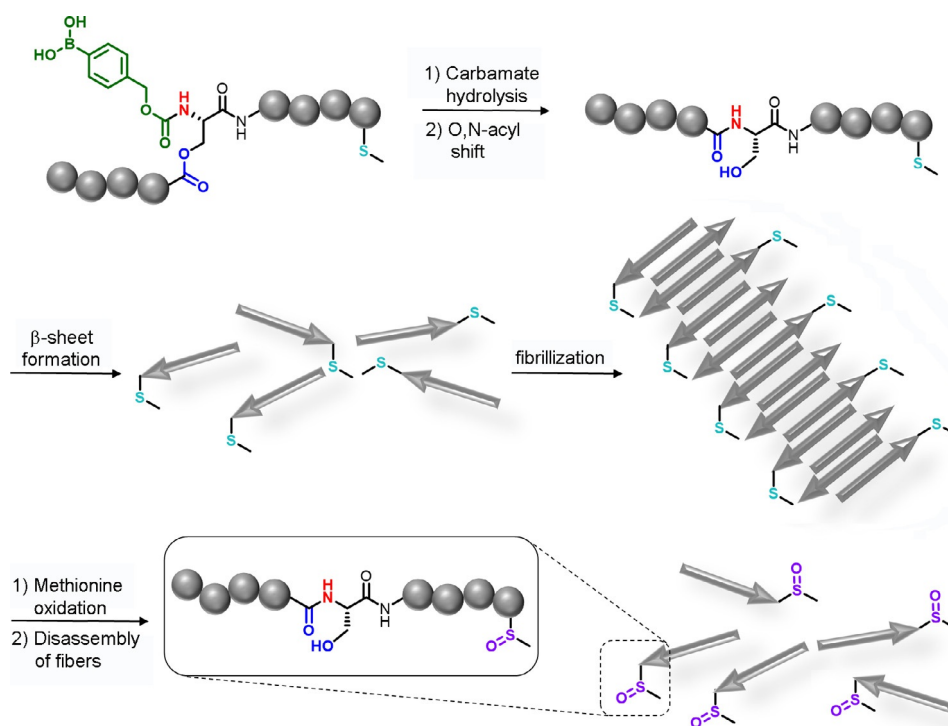


**Figure 1.** Chemical design and structure of a depsi-oligopeptide controlled by a boronic acid carbamate bond. The carbamate and methionine provide the two orthogonal stimuli.

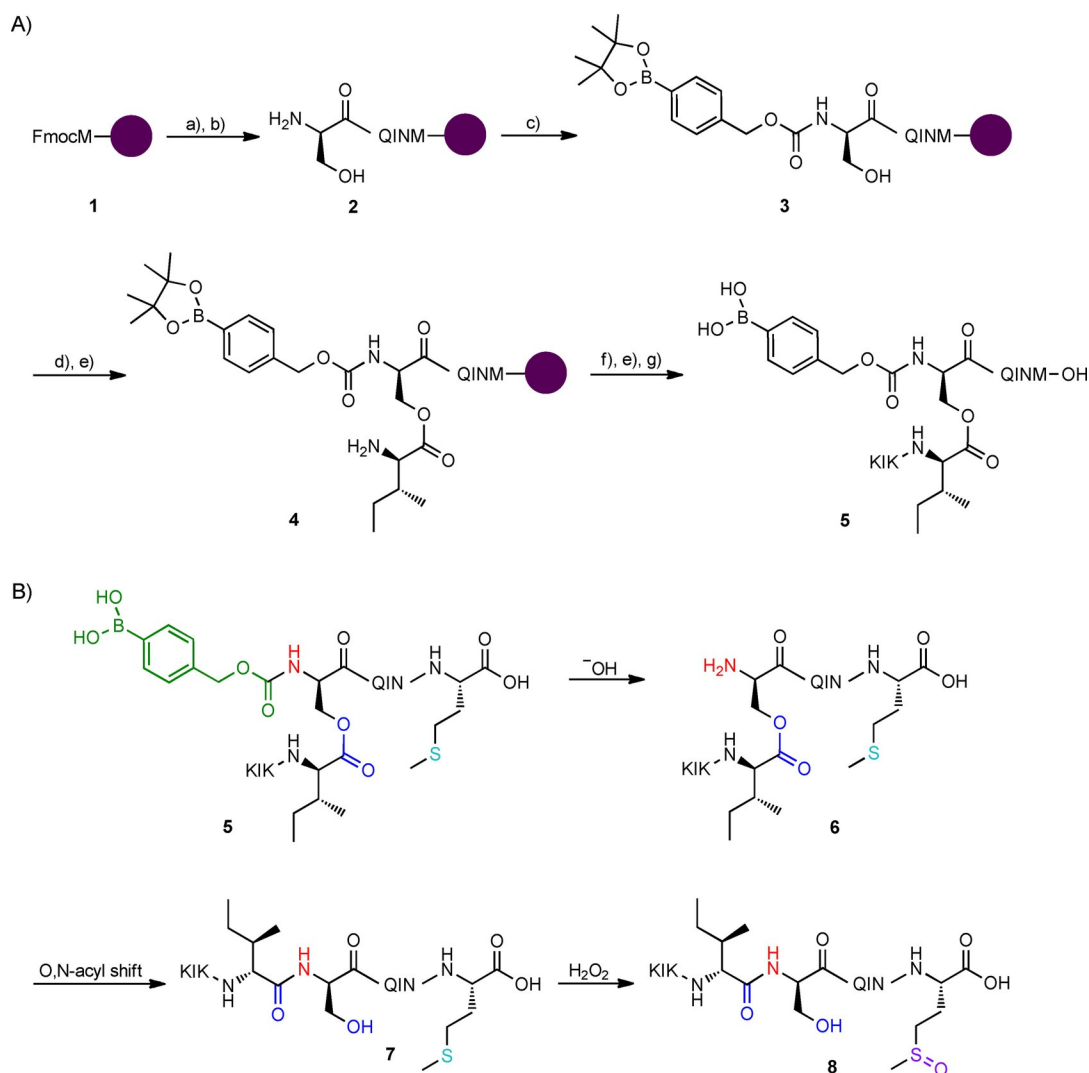
due in which the thioether motif directly imparts sensitivity to local oxidative conditions. In particular, an oxidative stimulus is attractive as it is well known that cancerous tissues contain a much higher concentration of hydrogen peroxide and various reactive oxygen species.<sup>[12]</sup> By integrating both aspects, amyloid self-assembly is directly controlled by the cleavage of the carbamate bond, whereas the disassembly is dictated by the oxidation of the methionine at the C terminus. In addition, the effects of these triggers produce distinct morphological changes that can be visualized by transmission electron microscopy (TEM). In establishing this concept, we anticipate that the methodology will provide enormous synergy with existing amyloid-based technology ranging from hydrogels<sup>[13]</sup> to drug delivery<sup>[14]</sup> and viral gene transduction.<sup>[5b]</sup>

David Ng studied chemistry at the National University of Singapore (B.Sc., first-class honours) followed by a doctorate with Prof. Dr. Tanja Weil jointly funded by the Max Planck Institute for Polymer Research and Ulm University (Dr. rer. nat., summa cum laude). After graduating in 2014, he began his career as a junior group leader at Ulm University and accepted his current position in 2016. He leads the group for synthetic life-like nanosystems focusing on using organic and polymer chemistry to instil synthetic functions into the architectures of peptides, proteins and DNA.



The synthesis of the oligopeptide takes place in the solid phase on Wang resin preloaded with the first amino acid, methionine (1). Standard microwave-assisted peptide synthesis was used to construct the peptide in sequence with asparagine, isoleucine and glutamine by using double coupling steps. Following this, 9-fluorenylmethoxycarbamate (Fmoc)-Ser-OH (Scheme 1) was coupled in a single step—in order to prevent side reactions with the free hydroxy group—to form 2. The Fmoc group was removed, then a boronic acid-carbamate caging group was installed by using 4-nitrophenyl(4-(4,4,5,5-tetramethyl-1,3,2-dioxaborolan-2-yl)benzyl)carbonate with *N,N*-diisopropylethylamine in DMF at room temperature overnight. The depsi-ester bond from the serine was constructed by treating 3 with Fmoc-Ile-OH, diisopropylcarbodiimide (DIC) and 4-dimethylaminopyridine (DMAP) to afford 4. The coupling of the next three residues—lysine, isoleucine and lysine—was conducted at room temperature as the carbamate bond is heat sensitive. Cleavage of the peptide, together with complete deprotection with 95% trifluoroacetic acid (TFA), 2.5% TIPS and 2.5% water afforded the target caged-oligopeptide 5.

The responsiveness of oligopeptide 5 towards the assembly trigger rests upon the boronic acid-carbamate caging group. Benzylic carbamate bonds are sensitive to hydrolytic conditions, and their stability can be tuned over a wide range, depending on the aromatic substituents.<sup>[15]</sup> Boronic acid was chosen both as an electron-withdrawing group and as a potential reactive chemical function. Hence, the experiment was designed to monitor the mechanism of bond cleavage by kinetic profiling using analytical HPLC (Figure 2A and Figure S5



**Scheme 1.** A) Microwave assisted solid-phase peptide synthesis of the target boronic acid caged depsipeptide **5**. a) Piperidine/DMF, 75 °C, 2 and 5 min; b) Fmoc-Asn(Trt)-OH/Fmoc-Ile-OH/Fmoc-Gln(Trt)-OH/Fmoc-Ser-OH, PyBOP, DIPEA, 75 °C, 2 × 10 min for Asn Ile, and Gln, 10 min for Ser; c) 4-nitrophenyl (4-(4,4,5,5-tetramethyl-1,3,2-dioxaborolan-2-yl)benzyl) carbonate, DIPEA, RT, overnight; d) Fmoc-Ile-OH, DIC, DMAP, RT, 2 h and overnight; e) piperidine, RT, 2 × 10 min; f) Fmoc-Ile/Fmoc-Lys(Boc)-OH, PyBOP, DIPEA, RT, 2 × 60 min; g) TFA, TIPS, water, RT, 2 h. B) Mechanism of stimulus-responsive O,N-acyl rearrangement of **5** and subsequent oxidation of methionine.

in the Supporting Information). We found that the carbamate bond can be cleaved selectively in the presence of kosmotropic agents such as phosphate salts, but is stable in pure water. A retention time of 11.0 min was observed for the caged peptide **5**. Gradual hydrolysis of the carbamate bond is observed over time, with the intermediate free depsipeptide **6** being formed at 10.3 min. It is important to note that **6** can be observed to undergo rapid O,N-acyl shift to form the linear peptide **7** at 10.2 min. After 24 h, full conversion to the linear peptide form was attained, although its formation and spontaneous self-assembly had already begun after 1 h (Figure S5). In order to confirm the peak assignments, oligopeptides **6** and **7** were synthesised separately and analysed as controls in the HPLC (Figure S5).

In a similar fashion, disassembly through the oxidation of methionine by applying H<sub>2</sub>O<sub>2</sub> was monitored (Figures 2B and S6). The final and linear forms of **7** were treated with 100 mM

H<sub>2</sub>O<sub>2</sub>. Oxidation of the thioether into a sulfoxide was apparent from the HPLC within 5 min (Figure 2B). A significant shift in the retention time towards higher polarity from 10.2 to 9.4 min was observed; this is in agreement with the formation of the more polar sulfoxide functional group. The conversion was about 85% within 1 h and was shown to be complete within 8 h.

Although the HPLC studies show definitive changes in the oligopeptide structure in response to both orthogonal stimuli, a molecular-level characterization would reinforce these observations. To this end, we used MALDI-TOF-MS to elucidate the peak identities (Figures 2C–E and S7). The loss of the carbamate caging motif from oligopeptide **5** ( $m/z$ : 1234.68 [ $M-H_2O+H$ ]<sup>+</sup>) could be correlated to the linear peptide **7** ( $m/z$ : 1074.45 [ $M+H$ ]<sup>+</sup>, 1096.43 [ $M+Na$ ]<sup>+</sup>). As the molecular weights of **6** and **7** are identical, characterization by MALDI-TOF MS is not possible. However, the transient presence of a

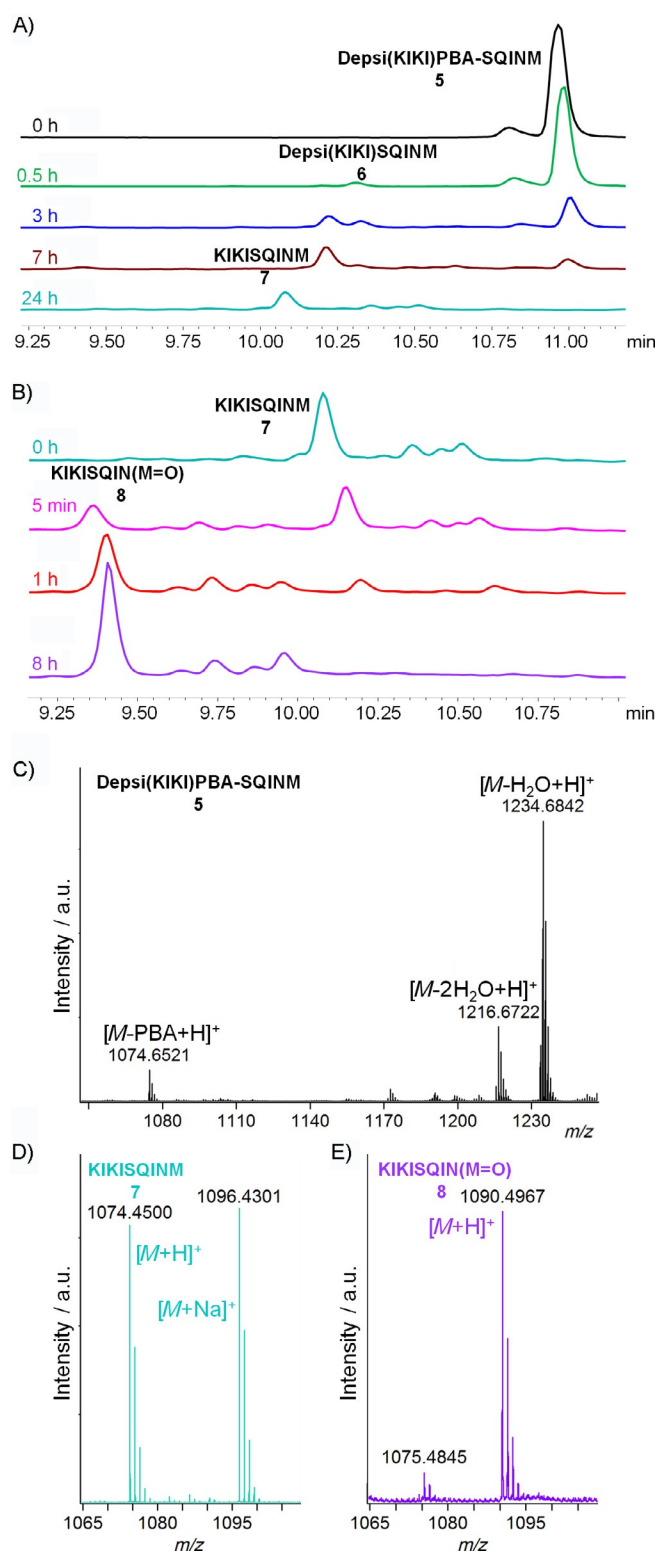


**Figure 2.** Kinetic profiling of A) hydrolysis of boronic acid-carbamate **5** with subsequent O,N-acyl rearrangement into **7** and B) oxidation of **7** by H<sub>2</sub>O<sub>2</sub>. MALDI-TOF-MS of C) Depsipeptide **5**, D) linearized peptide **7** and E) Oxidation of **7** into **8** by H<sub>2</sub>O<sub>2</sub>.

peak at  $t_R = 10.3$  min correlates to the well-reported rapid O,N-acyl shift of depsipeptide **6**.<sup>[9]</sup> In a complementary fashion, oxidation of oligopeptide **7** by H<sub>2</sub>O<sub>2</sub> was confirmed by the

addition of oxygen to form the sulfoxide **8** ( $m/z$ : 1090.50  $[M+H]^+$ ).

Upon the investigation of the molecular mechanisms, the self-assembling behaviour of caged depsipeptide **5** as a response towards both stimuli was elucidated. As the fundamental linear peptide sequence is known to form strong  $\beta$ -sheet supramolecular nanostructures, the rearrangement reaction could be characterized by Proteostat staining. The fluorogenic stain produced a large increase in fluorescence intensity upon triggering with phosphate salts, thus implying the responsive formation of  $\beta$ -sheet structures (Figures 3A and S8). In contrast, a control experiment containing the caged depsipeptide **5** in pure water did not show fluorescence upon staining. Subsequently, upon adding H<sub>2</sub>O<sub>2</sub> to **7** as the disassembly stimulus, the fluorescence diminished, thus implying the destruction of the cross- $\beta$ -sheet structures.

These results were further supported by performing FTIR and comparing these values to the known literature vibrational frequencies of the  $\beta$ -sheet peptidic assemblies.<sup>[16]</sup> Self-assembled peptide **7** showed distinct absorbances at 1635 and 1667 cm<sup>-1</sup>, which correspond to  $\beta$ -sheet structures and other secondary structures, respectively (Figures 3B and S9). Although the IR spectrum upon oxidation looks relatively similar it is important to note that the relative content of other non- $\beta$ -sheet structures is more significant. The higher absorbance at 1667 cm<sup>-1</sup> implies that  $\beta$ -sheet interactions are less dominant after the oxidation reaction. Hence, we speculate that the corresponding increase in other competing secondary structures is detrimental to self-assembly and interferes in the stability of the fibrillar structure. To support the results from IR, circular dichroism spectra of **5**, **7** and **8** were recorded (Figure S10). The spectrum of depsi(KIKI)PBA-SQINM **5** showed expected unordered structures, whereas KIKISQINM **7** was proven to form  $\beta$ -sheets. Upon oxidation of **7** to **8**, the spectrum changed considerably, with a reduction in  $\beta$ -sheet content and a corresponding increase in unordered structures (Figure S10, Table S1).<sup>[17]</sup>

To visualize our spectroscopic analysis, we performed transmission electron microscopy (TEM) of both the stimulated assembly of the depsipeptide and disassembly of the nanostructure (Figure 3C). Caged depsipeptide **5** was observed to spontaneously self-assemble into fibrillar nanostructures after hydrolysis of the carbamate bond in phosphate-buffered saline and subsequent rearrangement (Figure 3C). These nanofibres show the well-observed characteristic features of amyloid-like peptides that are known to build from continuous  $\beta$ -sheet interactions. The length of the fibres varies between around 100 nm and several micrometres. The diameter of the fibres is  $9.44 \pm 1.59$  nm, yet in some fibres the thickness can be observed to change periodically; this indicates twisting of the fibre strand along its axis. As can be seen in Figure S12, the twist is left-handed. Separated fibres as well as dense fibre networks can be observed. Some fibres are organised into multi-stranded assemblies, which appear a lot darker and thicker in TEM image than solitary fibres.<sup>[18]</sup> In agreement to other reports, a time-lapse study demonstrated that these nanofibres formed rapidly (1 h), with no observable increase in fibre densi-

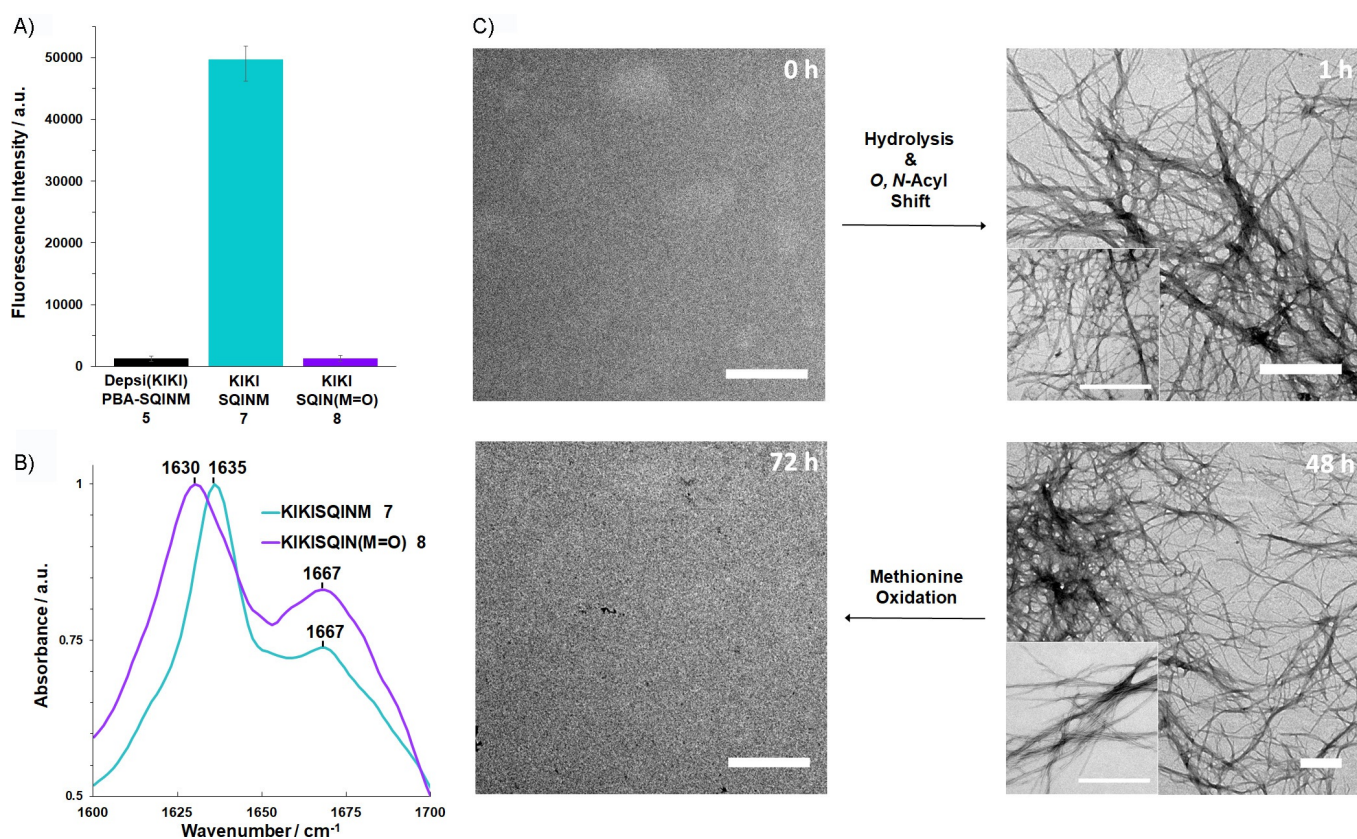


**Figure 3.** A) Proteostat assay of depsipeptide 5, hydrolysis of peptide 5 into 7 and oxidized peptide 8. Data are represented as mean  $\pm$  SEM,  $n=4$ . B) FTIR spectra of peptide 7 and oxidized peptide 8. C) TEM images of the O,N-acyl shift-triggered fibrillization (top) within 1 h. Complete disassembly of nanofibres by H<sub>2</sub>O<sub>2</sub> oxidation (bottom) over 24 h. Times are represented as cumulative intervals. Scale bars: 500 nm.

ty for the next 8 h (Figures S11, S13 and S14).<sup>[6a,8a]</sup> Subsequent oxidation with 100 mM H<sub>2</sub>O<sub>2</sub> successfully led to disassembly (Figure 3C).

The assembly of the peptides into  $\beta$ -sheets and further into nanofibres is based on an interplay of hydrogen bonds that are formed between the amide groups in the peptide backbone and hydrophobic interactions between the nonpolar amino acid side chains of isoleucine and methionine.<sup>[19]</sup> Additional stabilization of the structure is provided by hydrogen bonds formed by the side chains of glutamine and asparagine.<sup>[20]</sup> As shown by FTIR (Figure 3B), parallel  $\beta$ -sheets are formed; this is in accordance with Wang et al. who reported that peptides with strongly hydrophobic side chains form parallel rather than antiparallel  $\beta$ -sheets.<sup>[19c]</sup>

Oxidation of the nonpolar thioether in the methionine side chain to the corresponding sulfoxide significantly enhances the polarity of the side chain.<sup>[21]</sup> The dipolar character of sulfoxides is suspected to cause electrostatic repulsion between the methionine sulfoxide residues in the peptide side chains, and this leads to disassembly of the fibres.

In summary, we have presented a synthetic methodology that facilitates direct and independent control over the self-assembly of amyloid-like oligopeptides. Serine and methionine are necessary components of the design to implement the chemical triggers. Serine provides a unique handle to control the overall conformation of the peptidic backbone through

the depsi-ester bond, whereas methionine is sensitive to oxidation. Although the concentration of H<sub>2</sub>O<sub>2</sub> applied within this study still exceeds those in cancer environments, enzymatic triggers such as glucose oxidase could be combined—for example, in a hydrogel—to elevate local H<sub>2</sub>O<sub>2</sub> production as a response to glucose. Chemically, different caging groups that introduce other stimuli such as enzymes, light and pH could be tailored to fit a designated application. By providing this facile platform, we envision that control over self-assembly could be further extended beyond the peptide sequence.

## Acknowledgements

The authors gratefully acknowledge funding support from the Horizon 2020 project "AD GUT" (no. 686271) and from the Volkswagen Foundation Project 89943.

## Conflict of Interest

The authors declare no conflict of interest.

**Keywords:** amyloid peptides • nanostructures • rearrangement • self-assembly • stimulus-responsive assembly

- [1] D. B. Amabilino, D. K. Smith, J. W. Steed, *Chem. Soc. Rev.* **2017**, *46*, 2404–2420.
- [2] M. J. Webber, E. A. Appel, E. W. Meijer, R. Langer, *Nat. Mater.* **2016**, *15*, 13.
- [3] G. Wei, Z. Su, N. P. Reynolds, P. Arosio, I. W. Hamley, E. Gazit, R. Mezzenga, *Chem. Soc. Rev.* **2017**, *46*, 4661–4708.
- [4] I. W. Hamley, *Chem. Rev.* **2012**, *112*, 5147–5192.
- [5] a) D. Straßburger, N. Stergiou, M. Urschbach, H. Yurugi, D. Spitzer, D. Schollmeyer, E. Schmitt, P. Besenius, *ChemBioChem* **2018**, *19*, 912–916; b) M. Yolamanova, C. Meier, A. K. Shaytan, V. Vas, C. W. Bertoncini, F. Arnold, O. Zirafi, S. M. Usmani, J. A. Müller, D. Sauter, C. Goffinet, D. Palesch, P. Walther, N. R. Roan, H. Geiger, O. Lunov, T. Simmet, J. Bohne, H. Schrezenmeier, K. Schwarz, L. Ständker, W.-G. Forssmann, X. Salvatella, P. G. Khalatur, A. R. Khokhlov, T. P. J. Knowles, T. Weil, F. Kirchhoff, J. Münch, *Nat. Nanotechnol.* **2013**, *8*, 130.
- [6] a) Y. Liu, Y. Yang, C. Wang, X. Zhao, *Nanoscale* **2013**, *5*, 6413–6421; b) S. J. Sigg, V. Postupalenko, J. T. Duskey, C. G. Palivan, W. Meier, *Biomacromolecules* **2016**, *17*, 935–945; c) E. Lump, L. M. Castellano, C. Meier, J. Seeliger, N. Erwin, B. Sperlich, C. M. Stürzel, S. Usmani, R. M. Hammond, J. von Einem, G. Gerold, F. Kreppel, K. Bravo-Rodriguez, T. Pietschmann, V. M. Holmes, D. Palesch, O. Zirafi, D. Weissman, A. Sowislok, B. Wettig, C. Heid, F. Kirchhoff, T. Weil, F.-G. Klärner, T. Schrader, G. Bitan, E. Sanchez-Garcia, R. Winter, J. Shorter, J. Münch, *eLife* **2015**, *4*, e05397.
- [7] P. Ahlers, H. Frisch, R. Holm, D. Spitzer, M. Barz, P. Besenius, *Macromol. Biosci.* **2017**, *17*, 1700111.
- [8] a) J. Gačanin, J. Hedrich, S. Sieste, G. Glaßer, I. Lieberwirth, C. Schilling, S. Fischer, H. Barth, B. Knöll, C. V. Synatschke, T. Weil, *Adv. Mater.* **2019**, *31*, 1805044; b) A. Taniguchi, Y. Sohma, Y. Hirayama, H. Mukai, T. Kimura, Y. Hayashi, K. Matsuzaki, Y. Kiso, *ChemBioChem* **2009**, *10*, 710–715.
- [9] I. Coin, R. Dölling, E. Krause, M. Bienert, M. Beyermann, C. D. Sferdean, L. A. Carpino, *J. Org. Chem.* **2006**, *71*, 6171–6177.
- [10] L. Sun, C. Zheng, T. J. Webster, *Int. J. Nanomed.* **2016**, *12*, 73–86.
- [11] A. Dehsorkhi, V. Castelletto, I. W. Hamley, *J. Pept. Sci.* **2014**, *20*, 453–467.
- [12] C. Lennicke, J. Rahn, R. Lichtenfels, L. A. Wessjohann, B. J. C. C. Seliger, *Cell Commun. Signal.* **2015**, *13*, 39.
- [13] S. Das, K. Zhou, D. Ghosh, N. N. Jha, P. K. Singh, R. S. Jacob, C. C. Bernard, D. I. Finkelstein, J. S. Forsythe, S. K. Maji, *NPG Asia Mater.* **2016**, *8*, e304.
- [14] N. Habibi, N. Kamaly, A. Memic, H. Shafiee, *Nano Today* **2016**, *11*, 41–60.
- [15] A. K. Ghosh, M. Brindisi, *J. Med. Chem.* **2015**, *58*, 2895–2940.
- [16] G. Zandomenighi, M. R. H. Krebs, M. G. McCammon, M. Fändrich, *Protein Sci.* **2004**, *13*, 3314–3321.
- [17] a) Y. Liu, L. Zhang, W. Wei, *Int. J. Nanomed.* **2017**, *12*, 659–670; b) R. Xing, C. Yuan, S. Li, J. Song, J. Li, X. Yan, *Angew. Chem. Int. Ed.* **2018**, *57*, 1537–1542; *Angew. Chem.* **2018**, *130*, 1553–1558.
- [18] K. Pagel, S. C. Wagner, K. Samedov, H. von Berlepsch, C. Böttcher, B. Kokschi, *J. Am. Chem. Soc.* **2006**, *128*, 2196–2197.
- [19] a) K. Liu, R. Xing, C. Chen, G. Shen, L. Yan, Q. Zou, G. Ma, H. Möhwald, X. Yan, *Angew. Chem. Int. Ed.* **2015**, *54*, 500–505; *Angew. Chem.* **2015**, *127*, 510–515; b) N. R. Lee, C. J. Bowerman, B. L. Nilsson, *Biomacromolecules* **2013**, *14*, 3267–3277; c) J. Wang, K. Liu, R. Xing, X. Yan, *Chem. Soc. Rev.* **2016**, *45*, 5589–5604; d) C. Yuan, S. Li, Q. Zou, Y. Ren, X. Yan, *Phys. Chem. Chem. Phys.* **2017**, *19*, 23614–23631.
- [20] S. Sieste, T. Mack, C. V. Synatschke, C. Schilling, C. Meyer zu Reckendorf, L. Pendi, S. Harvey, F. S. Ruggeri, T. P. J. Knowles, C. Meier, D. Y. W. Ng, T. Weil, B. Knöll, *Adv. Healthcare Mater.* **2018**, *7*, 1701485.
- [21] D. Spitzer, L. L. Rodrigues, D. Straßburger, M. Mezger, P. Besenius, *Angew. Chem. Int. Ed.* **2017**, *56*, 15461–15465; *Angew. Chem.* **2017**, *129*, 15664–15669.

Manuscript received: December 10, 2018

Accepted manuscript online: January 28, 2019

Version of record online: April 12, 2019